

pubs.acs.org/NanoLett Letter

The Stark Effect: A Tool for the Design of High-Performance Molecular Rectifiers

Ryan P. Sullivan, John T. Morningstar, Eduardo Castellanos-Trejo, Mark E. Welker, and Oana D. Jurchescu*



Cite This: Nano Lett. 2023, 23, 10864-10870



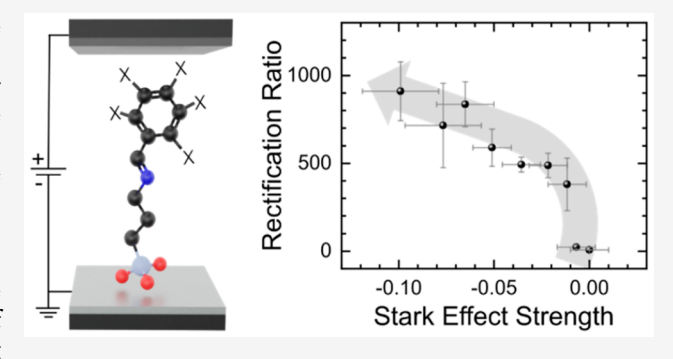
ACCESS

Metrics & More

Article Recommendations

s Supporting Information

ABSTRACT: Molecular electronic devices offer a path to the miniaturization of electronic circuits and could potentially facilitate novel functionalities that can be embedded into the molecular structure. Given their nanoscale dimensions, device properties are strongly influenced by quantum effects, yet many of these phenomena have been largely overlooked. We investigated the mechanism responsible for current rectification in molecular diodes and found that efficient rectification is achieved by enhancing the Stark effect strength and enabling a large number of molecules to participate in transport. These findings provided insights into the operation of molecular rectifiers and guided the development of high-performance devices via the design of molecules containing



polarizable aromatic rings. Our results are consistent for different molecular structures and are expected to have broad applicability to all molecular devices by answering key questions related to charge transport mechanisms in such systems.

KEYWORDS: molecular rectifiers, Stark effect, charge transport, charge injection, self-assembly

olecular electronic devices use molecules as the basic VI building blocks and have the potential to revolutionize the way electronic circuits are designed and manufactured. Their properties can be tailored by modifying the chemical structure of molecules used, and hence, they are quickly expanding into novel functionalities, including optical photoswitches, synaptic-emulating memristors, chemical and biological sensors,^{3–5} and wires with tunable conductivity,⁶ all of which offer nanoscale and cost-efficient functionality to complement conventional technologies. One of the simplest molecular devices—the molecular rectifier—consists of a single molecule or a self-assembled monolayer (SAM) sandwiched between two contacts that acts as a conductor under forward bias and as an insulator under the opposite bias, allowing current to effectively flow only in one direction. The efficiency in current rectification is quantified by the rectification ratio, $R = |J(V^+)/J(V^-)|$, defined as the ratio between current density J under forward bias (V^{+}) and the current density under the reverse bias of the same magnitude, $J(V^{-})$. This device was theoretically proposed in 1974⁷ and first demonstrated experimentally in the early 1990s, 8-10 with substantial improvements in performance being achieved within the past decade; several groups have reported rectification ratios of 10^2-10^3 , and values of >105 have also been demonstrated. 11-18 The rectification process has largely been explained by intramolecular donor-acceptor mechanisms (Aviram and Ratner ansatz) and asymmetric tunneling through

one or more frontier molecular orbitals. 7,19-21 Introducing asymmetry into molecular rectifiers has been achieved by gate effects, 13 asymmetric molecule/electrode coupling, 22,23 interaction with the environment,³ and, more recently, the Stark effect.²⁴⁻²⁶ The Stark effect is a quantum phenomenon that describes the splitting and shifting of the energy levels within atoms or molecules when subjected to a strong electric field, similar to the Zeeman effect occurring in the presence of a magnetic field.^{27–31} The magnitude of the shift depends on the strength and orientation of the electric field as well as the difference between the excited and ground state dipole moments. Typically, Stark shift measurements are modeled by linear and quadratic shifts with an applied bias and are often used to investigate the polarizability of atoms and molecules.²⁹ In molecular rectifiers, the Stark effect has been adopted to describe how an applied electric field shifts the energies of the molecular orbitals to induce asymmetric tunneling, which yields current rectification. ^{24–26} There are a number of theories about the Stark effect in molecular electronics; however, its role in high-performance molecular rectifiers and

Received: August 15, 2023 Revised: November 10, 2023 Accepted: November 13, 2023

Published: November 16, 2023





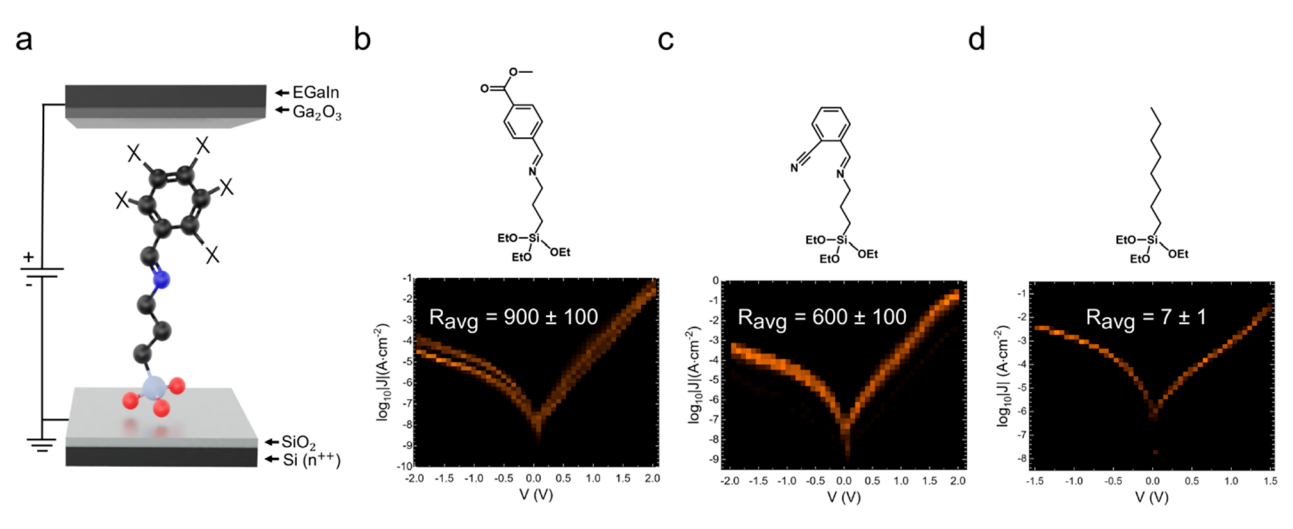


Figure 1. (a) Device structure of the molecular junctions. (b-d) Chemical structures and corresponding current—voltage characteristics sorted into 2D bins for molecules 1 (panel b), 2 (panel c) and 3 (panel d).

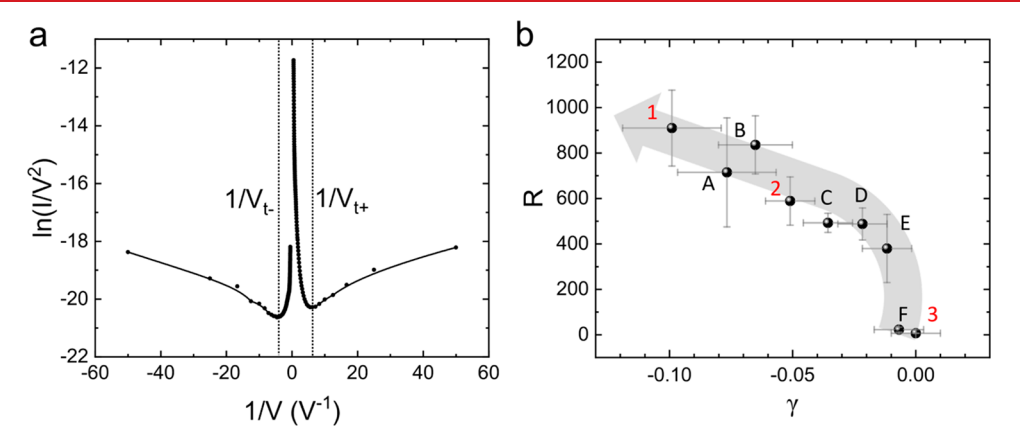


Figure 2. (a) Example Fowler–Nordheim plot used to determine the transition voltage of each molecular junction. (b) Average R with the standard deviation vs γ for the nine different molecular compounds investigated.

its relationship to molecular structure are not yet clear. A deeper understanding of this phenomenon will not only shed light on the mechanism of charge transport at molecular length scales but also be essential for the advancement of other molecular technologies. Here, we investigate the Stark effect in a large set of molecular rectifiers that exhibit rectification ratios spanning several orders of magnitude, from lower than 10 to greater than 10³. Through transition voltage spectroscopy, we found a positive correlation between the Stark effect strength and the rectification ratio, suggesting that the Stark effect plays a significant role in the operation of molecular rectifiers. We employed an expanded Landauer-Büttiker expression utilizing a first-order approximation for the Stark effect strength and assumed an exponential dependence of the number of molecules participating in transport on the applied voltage to effectively model the current-voltage characteristics by using experimentally derived properties as key fitting parameters. We found that the current rectification is more effective in molecular rectifiers based on SAMs containing aromatic functional groups with polar substituents due to synergistic effects of a more pronounced shift in the molecular orbitals (Stark effect) and a larger number of molecules participating in transport.

To fabricate the devices, we started from degenerately doped n-type silicon substrates (resistivity of 0.001–0.005 Ω cm)

with an ~2 nm native oxide layer, which have been cleaned for 10 min in an acetone bath at 85 °C, followed by an acetone and isopropyl alcohol (IPA) rinse and a 10 min IPA bath at 85 °C. Then they were blown dry under nitrogen, exposed to ultraviolet ozone for 10 min, rinsed with deionized water, and dried again under a stream of nitrogen. Next, the substrates were placed in glass containers inside a nitrogen glovebox, where they were immersed into a 7 mM solution of SAM in room-temperature chloroform for ~16-20 h allowing ample time for self-assembly. Afterward, the samples were thoroughly rinsed with chloroform and then IPA and finally dried again under nitrogen. The molecular structures of the SAMs are illustrated in Figure S1; they consist of a triethoxysilane anchoring group with various functionalized tails that are electrically decoupled by an insulating σ -bonded bridge. ^{18,23} Molecular junctions were formed with close to 100% yields by utilizing a non-invasive top contact of EGaIn (eutectic gallium-indium), which contains a thin (~0.7 nm) Ga₂O₃ (gallium oxide) layer that spontaneously forms on its surface, creating a metal/oxide/SAM/oxide/metal device architecture. 14,32-34 A schematic of the device structure is included in Figure 1a. By using silicon substrates with soft top contacts, we emphasize cost-efficient device processing by avoiding expensive evaporation and/or template-stripping processes.^{3,14,35}

Nano Letters pubs.acs.org/NanoLett Letter

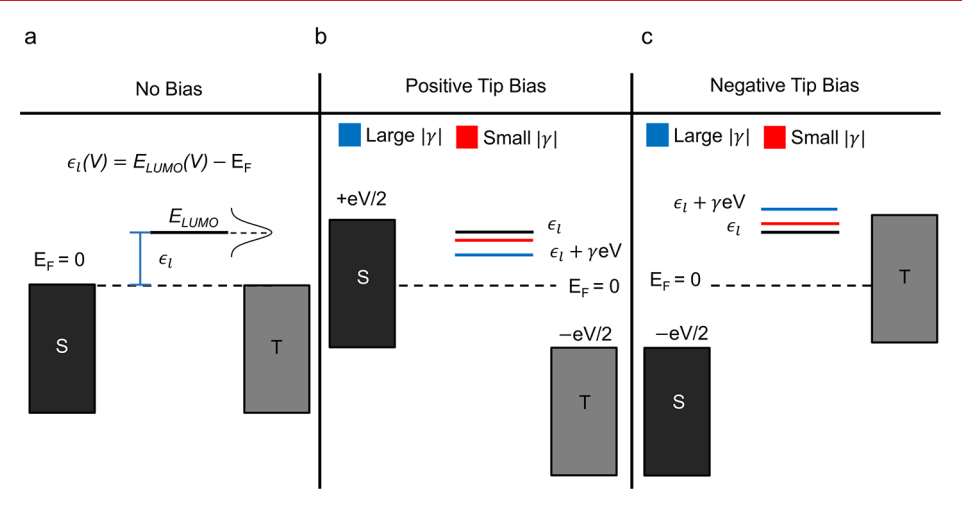


Figure 3. Energy level diagram illustrating the rectification mechanism resulting from the LUMO being asymmetrically shifted by the Stark effect. The panels correspond to (a) no applied bias and (b) a positive LUMO shift outside the transmission window. This is in agreement with the data displayed in Figure S5, where the measured value of the negative current exponentially decreases with $|\gamma|$, whereas the positive current only slightly increases and then decreases (overall remaining relatively constant), leading to the observed increase in R in Figure 2b.

Rectification ratio R was determined by electrically characterizing the molecular rectifiers under ambient conditions using an Agilent 4155C semiconductor parameter analyzer and performing voltage sweeps from 0 to 2 V, followed by 0 to -2 V to minimize any potential hysteresis effects that could influence the experimental outcome and complicate the analysis. The results obtained for (E)-1-(4carbomethoxy-phenyl)-N-[3-(triethoxysilyl)propyl]methanimine, (E)-1-(3-cyanophenyl)-N-[3-(triethoxysilyl)propyl methanimine, and triethoxy(octyl)silane, which are labeled as molecules 1-3, respectively, are illustrated in panels b-d, respectively, of Figure 1, alongside the molecular structures. The measured current-voltage characteristics were assorted into two-dimensional (2D) bins, which show highly consistent curves indicative of ordered films. The corresponding rectification ratio histograms are shown in Figure S2. These examples correspond to molecular rectifiers exhibiting high, medium, and low rectification ratios within the set of devices we investigated. Similar measurements were performed for all nine different SAMs, producing R values from 5 to 1100; the results are shown in Figure S3. Note that rectification ratios as high as 9000 can be obtained in some of these SAMs upon co-assembly of molecules in which donoracceptor interactions can occur, resulting in new electronic states. 18 Nevertheless, here, we restricted our study to monomolecular SAMs to avoid the contribution of charge transfer states, which would have complicated the interpretation of the results.

Transition voltage spectroscopy (TVS) was used to determine transition voltage $V_{\rm t}$. The Fowler–Nordheim plot $[\ln(I/V^2) \text{ vs } 1/V]$ was generated on the basis of the current–voltage characteristics measured on each device, and $V_{\rm t}$ was extracted as the voltage at the minimum of this plot (Figure 2a), where $V_{\rm t+}$ ($V_{\rm t-}$) corresponds to the minimum in the positive (negative) bias regime. Transition voltages were determined by using the averaged I-V curves corresponding to the measurements illustrated in Figure S2. All reported R values correspond to $V=\pm 2$ V, except for the case of molecule 3 where R was measured at ± 1.5 V due to electrical breakdowns at higher voltages. Upon adoption of the single-level model, the energy offset between the LUMO (lowest unoccupied molecular orbital) level and the Fermi energy ($E_{\rm E}$)

is defined as $\varepsilon_{\rm l}$ = $E_{\rm LUMO}$ – $E_{\rm F}$. ³⁷ In a junction under an external bias, the LUMO shifts proportionally with respect to applied voltage V

$$E_{\text{LUMO}}(V) = E_{\text{LUMO}} + \gamma eV \tag{1}$$

where e represents the elementary charge and Stark effect strength (orbital shift) γ is determined by

$$\gamma = \frac{1}{2} \frac{V_{t+} + V_{t-}}{\sqrt{V_{t+}^2 + 10|V_{t+}V_{t-}|/3 + V_{t-}^2}}$$
(2)

 ε_1 is also dependent on voltage, such as

$$\varepsilon_{l}(V) = E_{LUMO}(V) - E_{F} = \varepsilon_{l} + \gamma eV$$
 (3)

where ε_1 corresponds to the energy offset in the absence of an applied voltage.

In the following, we focus on determining the Stark effect strength for each molecule and assessing whether there is a dependence of R on this parameter. Small adjustments were made to the measured V_t to account for the asymmetric electrodes (the respective work functions of the EGaIn and silicon electrodes are -4.2 and -4.65 eV, respectively) (details included in Figure S4). As shown in Figure 2b, a positive trend between $|\gamma|$ and R exists, with R being very small for low values of γ and a significant jump in R occurring around $|\gamma| = 0.02$, followed by a less steep increase at a higher γ . The magnitude of γ is modulated by the Stark effect and the asymmetric location of the orbital in the junction, and the values shown in Figure 2b should be viewed as an underestimation due to contact effects, which result in screening of the applied electric field by the trap states forming at the molecule-electrode interface. This phenomenon, in turn, will indirectly impact the current rectification by reducing the magnitude of the effective voltage shifting the HOMO/LUMO level within the SAM.³⁸ For reference, a maximum rectification ratio of ~500 was predicted when considering only the contribution of the Stark effect to the rectification.³⁸ We note that other effects such as the internal molecular dipole, asymmetric placement of the orbital in the junction, or the length of the molecules also contribute to the rectification ratio and will impact the data depicted in Figure 2b.35 It is essential to discuss this experimental observation in a broader context. The clear

Nano Letters pubs.acs.org/NanoLett Letter

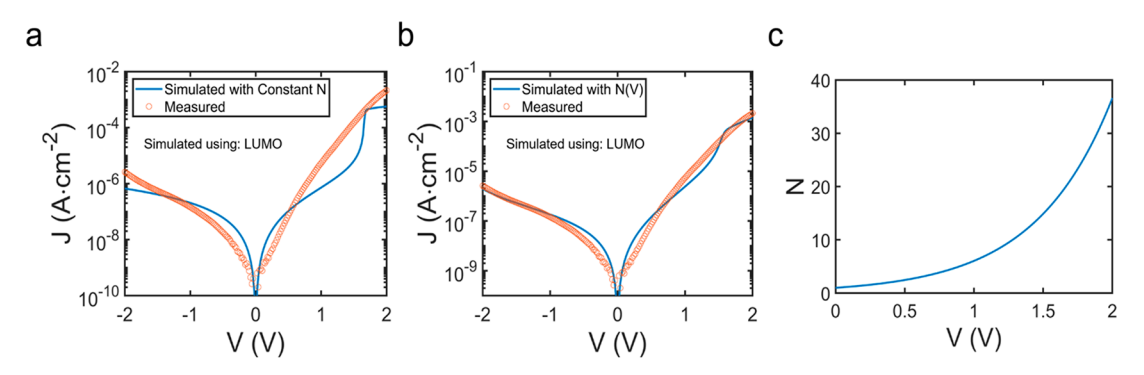


Figure 4. Average current—voltage characteristics of molecule 1 fitted to a Landauer—Büttiker expression (eq 8) when using (a) a constant N and (b) an N(V) that exponentially depends on the applied bias. (c) The relative N(V) was determined from the best fit.

dependence of R on γ suggests that the Stark effect is a key phenomenon in molecular electronics that could potentially be controlled for the development of new and improved devices. Another important observation is that both R and $|\gamma|$ are larger in SAMs containing aromatic rings, in agreement with previous reports that found that aromaticity increases the extent of molecular rectification. However, there is no clear correlation of $|\gamma|$ with the electronegativity of the substituent to the aromatic ring, where other effects like the degree of order within the SAM, coupling with the electrodes, or intermolecular interactions are likely playing a role.

Having established the positive correlation between γ and R, we can now describe the rectification mechanism in the presence of the Stark effect. In Figure 3, we focus on two cases, i.e., large and small γ values, depicted in blue and red, respectively. Figure 3a corresponds to the energy level diagram in the absence of an external bias, where S and T are the energy levels of the substrate (bottom electrode) and the top electrode, respectively. Assuming that the facilitating orbital is the LUMO for all investigated molecules, according to eq 1, if γ < 0, such as in the case of our devices, a positive (negative) bias shifts the frontier orbitals downward (upward), with the magnitude of the shift being proportional to γ and applied voltage V (Figure 3b,c). A positive bias shifts the LUMO level closer to $E_{\rm F}$; the larger the value of $|\gamma|$, the smaller the voltage needed to reach resonance (see eq 3). The current gradually increases until it reaches resonance and then decreases until the next energetic level participates in transport. On the contrary, when a negative bias is applied, the LUMO shifts further from $E_{\rm F}$, reducing the current and even placing the LUMO above the top electrode for large $|\gamma|$ values, yielding a significant decrease in the current when the LUMO shifts outside the transmission window. This is in agreement with the data displayed in Figure S5, where the measured value of the negative current exponentially decreases with $|\gamma|$, whereas the positive current only slightly increases and then decreases (overall remaining relatively constant), leading to the observed increase in *R* in Figure 2b.

We further examined the implications of our findings by employing the Landauer–Büttiker theory, which has been extensively used when simulating current–voltage characteristics in molecular devices. ^{24,25,40–42} In the framework of this theory, the current through molecular assemblies can be modeled by summing over the transmission probabilities of possible conduction channels:

$$I(V) = \frac{2Ne}{h} \int_{-\infty}^{\infty} dE T(E; V) [f_{T}(E; V) - f_{S}(E; V)]$$
 (4)

where N is the number of conducting molecules, E is the energy, $f_{\rm T}$ and $f_{\rm S}$ are the Fermi functions of the top electrode and bottom electrode (substrate), respectively, and T is the transmission function. The transmission function is expressed as

$$T(E) = \frac{4\Gamma_{\rm S}\Gamma_{\rm T}}{4(E - E_{\rm LUMO})^2 + (\Gamma_{\rm S} + \Gamma_{\rm T})^2}$$
 (5)

where $\Gamma_{\rm T}$ ($\Gamma_{\rm S}$) is the level broadening due to the molecule–electrode coupling for the top electrode (substrate). We will account for a linearly approximated shift of $\varepsilon_{\rm l}(V)$ by including a Stark effect strength coefficient described by eq 3, leading to the transmission function:

$$T(E) = \frac{4\Gamma_{\rm S}\Gamma_{\rm T}}{4(E - E_{\rm LUMO} - \gamma eV)^2 + (\Gamma_{\rm S} + \Gamma_{\rm T})^2}$$
(6)

When the temperature effects are ignored, the Fermi functions become steplike functions, allowing the integral to be analytically solved.

$$I(V) = \frac{2Ne}{h} \int_{E_{\rm F} - eV/2}^{E_{\rm F} + eV/2} dET(E; V)$$
 (7)

such that

$$I = \frac{4Ne\Gamma_{\rm S}\Gamma_{\rm T}}{h(\Gamma_{\rm S} + \Gamma_{\rm T})} \left\{ \arctan \left[\frac{\varepsilon_{\rm L} + \left(\gamma + \frac{1}{2}\right)eV}{(\Gamma_{\rm S} + \Gamma_{\rm T})/2} \right] - \arctan \left[\frac{\varepsilon_{\rm L} + \left(\gamma - \frac{1}{2}\right)eV}{(\Gamma_{\rm S} + \Gamma_{\rm T})/2} \right] \right\}$$

$$(8)$$

Figure 4a shows the current—voltage characteristics measured on molecule 1 (red circles) along with the curve generated using the expression in eq 8 (free fitting parameters included $\varepsilon_{\rm l}$, γ , $\Gamma_{\rm S}$, $\Gamma_{\rm T}$, and N), shown in blue, with small adjustments to account for the asymmetric contacts; details about the fitting parameters are included in Table S1. In spite of our attempts to model the experimental curves with this expression, even when using multiple molecular orbitals along with γ values that are significantly larger than the experimental results, the fit was still not satisfactory (Figure S6), suggesting that additional effects must be considered. Similar results have been obtained for molecules 2 and 3 (Figure S7a,b). The underestimation of the current values at high forward voltages prompted us to further consider the dependence of the number of molecules participating in transport on the applied

bias, N(V). A bias-dependent N has been previously used when modeling high-performance molecular rectifiers. ¹⁴ Here, for the first time, we integrate this concept with the Landauer formalism. Indeed, modeling the same experimental currentvoltage characteristics with the expression in eq 8, while using the exponential dependence of N on the applied bias, not only resulted in good agreement with the experimental points but also allowed us to use the experimentally derived Stark effect strength and removed the need for any molecular orbitals other than the LUMO (free fitting parameters include $\varepsilon_{\rm b}$ $\Gamma_{\rm S}$, $\Gamma_{\rm T}$, and N); the results are shown in Figure 4b, with details on the fitting parameters included in Table S1. The corresponding fits for molecules 2 and 3 are included in panels c and d of Figure S7, and the dependence of the relative N on V [the relative N(V) is normalized by N when V = 0 is shown in Figure 4c for molecule 1 and panels e and f of Figure S7 for the other molecules. The dependence of N on V also resulted in a significantly better agreement when fitting to the average rectification ratio versus voltage data (Figure S8). Upon comparison of the values of N for molecules 1-3, one can observe that in SAMs that exhibit a high rectification ratio the N at V = 2 V is ~30 times larger than the N at $V \sim 0$ V, while in the low rectifying SAMs, N(V) remains close to unity. The N(V) dependence in the highly rectifying SAMs is similar to that of previously reported molecular rectifiers based on thiols assembled on gold substrates. 14 This difference in N(V) values in our samples is attributed to the molecular structures of the tail groups. Specifically, the tail group of molecule 3 is a nonpolar, insulating, aliphatic chain leading to negligible changes in N with an increase in voltage, whereas the substituted aromatic compounds such as molecules 1 and 2 are polarizable, which allows the molecules to charge and reconfigure on the basis of an applied bias. These findings suggest that polar substituents can enhance molecular rectification. Because the coupling with one of the electrodes can also have an effect on the magnitude of the rectification ratio, 22,23 we also evaluated the average Γ for each molecule through zero-bias conductivity measurements.²⁴ However, we observed no statistically relevant relationship between R and Γ , confirming that the Stark effect, and not asymmetric-electrode coupling, is dominating the rectification mechanism in our devices. 43 We also attempted to model the experimental points obtained on molecule 1 when assuming charge transport through multiple molecular orbitals, where the total current through the molecule is a summation of all of the contributing orbitals determined from eq 8. We used two different molecular orbital combinations to explore if better fits could be obtained; the additional fits consisted of the HOMO and LUMO as well as the HOMO, LUMO, and LUMO+1 (Figure S9a,b). However, no significant improvements were noted, further confirming that the charge transport in our SAMs is dominated by a single molecular orbital. The corresponding voltage dependencies of the rectification ratios are illustrated in panels c and d of Figure S9.

In summary, we demonstrated that the Stark effect can significantly impact current rectification in molecular diodes by asymmetrically shifting the molecular orbitals participating in charge transport. By analyzing a large data set measured on molecules with rectification properties ranging from negligible to very strong, we have shown that the Stark effect strength correlates positively with the rectification ratio, with statistical significance. Using experimentally derived parameters, the current—voltage characteristics were successfully modeled with

a modified Landauer—Büttiker theory, which accounts for the voltage dependence of the number of molecules participating in transport. We found that polar conjugated aromatic compounds are more effective in current rectification as a result of a stronger Stark effect and a more pronounced dependence of the number of molecules participating in transport on the applied voltage. On the basis of these lessons, we have demonstrated high-performance molecular rectifiers with rectification ratios exceeding 10³ using cost-efficient materials and processing schemes that are also high throughput with nearly 100% yields. Our insights into charge transport mechanism in molecular rectifiers in molecular rectifiers are important for the development of high-performance organic—electronic devices.

ASSOCIATED CONTENT

Supporting Information

The Supporting Information is available free of charge at https://pubs.acs.org/doi/10.1021/acs.nanolett.3c03068.

Chemical structures, rectification ratio histograms, illustration of the transition voltage, current versus Stark effect strength, and additional modeling with a table of fitting parameters (PDF)

AUTHOR INFORMATION

Corresponding Author

Oana D. Jurchescu — Department of Physics and Center for Functional Materials, Wake Forest University, Winston-Salem, North Carolina 27109, United States; oorcid.org/0000-0003-2204-2909; Email: jurchescu@wfu.edu

Authors

Ryan P. Sullivan – Department of Physics and Center for Functional Materials, Wake Forest University, Winston-Salem, North Carolina 27109, United States; occid.org/0000-0001-8043-8376

John T. Morningstar – Department of Chemistry and Center for Functional Materials, Wake Forest University, Winston-Salem, North Carolina 27109, United States

Eduardo Castellanos-Trejo — Department of Physics and Center for Functional Materials, Wake Forest University, Winston-Salem, North Carolina 27109, United States

Mark E. Welker – Department of Chemistry and Center for Functional Materials, Wake Forest University, Winston-Salem, North Carolina 27109, United States

Complete contact information is available at: https://pubs.acs.org/10.1021/acs.nanolett.3c03068

Notes

The authors declare no competing financial interest.

ACKNOWLEDGMENTS

This work was partially supported by the National Science Foundation under Grants ECCS-1810273 and DMR-1627925.

REFERENCES

(1) Jia, C.; Migliore, A.; Xin, N.; Huang, S.; Wang, J.; Yang, Q.; Wang, S.; Chen, H.; Wang, D.; Feng, B.; Liu, Z.; Zhang, G.; Qu, D.-H.; Tian, H.; Ratner, M. A.; Xu, H. Q.; Nitzan, A.; Guo, X. Covalently Bonded Single-Molecule Junctions with Stable and Reversible Photoswitched Conductivity. *Science* 2016, 352 (6292), 1443–1445. (2) Wang, Y.; Zhang, Q.; Astier, H. P. A. G.; Nickle, C.; Soni, S.; Alami, F. A.; Borrini, A.; Zhang, Z.; Honnigfort, C.; Braunschweig, B.;

- Leoncini, A.; Qi, D.-C.; Han, Y.; del Barco, E.; Thompson, D.; Nijhuis, C. A. Dynamic Molecular Switches with Hysteretic Negative Differential Conductance Emulating Synaptic Behaviour. *Nat. Mater.* **2022**, *21* (12), 1403–1411.
- (3) Atesci, H.; Kaliginedi, V.; Celis Gil, J. A.; Ozawa, H.; Thijssen, J. M.; Broekmann, P.; Haga, M.; van der Molen, S. J. Humidity-Controlled Rectification Switching in Ruthenium-Complex Molecular Junctions. *Nat. Nanotechnol.* **2018**, *13* (2), 117–121.
- (4) Fuller, C. W.; Padayatti, P. S.; Abderrahim, H.; Adamiak, L.; Alagar, N.; Ananthapadmanabhan, N.; Baek, J.; Chinni, S.; Choi, C.; Delaney, K. J.; Dubielzig, R.; Frkanec, J.; Garcia, C.; Gardner, C.; Gebhardt, D.; Geiser, T.; Gutierrez, Z.; Hall, D. A.; Hodges, A. P.; Hou, G.; Jain, S.; Jones, T.; Lobaton, R.; Majzik, Z.; Marte, A.; Mohan, P.; Mola, P.; Mudondo, P.; Mullinix, J.; Nguyen, T.; Ollinger, F.; Orr, S.; Ouyang, Y.; Pan, P.; Park, N.; Porras, D.; Prabhu, K.; Reese, C.; Ruel, T.; Sauerbrey, T.; Sawyer, J. R.; Sinha, P.; Tu, J.; Venkatesh, A. G.; VijayKumar, S.; Zheng, L.; Jin, S.; Tour, J. M.; Church, G. M.; Mola, P. W.; Merriman, B. Molecular Electronics Sensors on a Scalable Semiconductor Chip: A Platform for Single-Molecule Measurement of Binding Kinetics and Enzyme Activity. *Proc. Natl. Acad. Sci. U. S. A.* 2022, 119 (5), No. e2112812119.
- (5) Sullivan, R. P.; Castellanos-Trejo, E.; Ma, R. E.; Welker, M. D.; Jurchescu, O. Humidity Sensors Based on Molecular Rectifiers. *Nanoscale* **2022**, *15* (1), 171–176.
- (6) Greenwald, J. E.; Cameron, J.; Findlay, N. J.; Fu, T.; Gunasekaran, S.; Skabara, P. J.; Venkataraman, L. Highly Nonlinear Transport across Single-Molecule Junctions via Destructive Quantum Interference. *Nat. Nanotechnol.* **2021**, *16* (3), 313–317.
- (7) Aviram, A.; Ratner, M. A. Molecular Rectifiers. *Chem. Phys. Lett.* **1974**, 29 (2), 277–283.
- (8) Geddes, N. J.; Sambles, J. R.; Jarvis, D. J.; Parker, W. G.; Sandman, D. J. Fabrication and Investigation of Asymmetric Current-Voltage Characteristics of a Metal/Langmuir-Blodgett Monolayer/Metal Structure. *Appl. Phys. Lett.* **1990**, *56*, 1916–1918.
- (9) Ashwell, G. J.; Sambles, J. R.; Martin, A. S.; Parker, W. G.; Szablewski, M. Rectifying Characteristics of Mgl(C16H33-Q3CNQ LB Film)|Pt Structures. *J. Chem. Soc., Chem. Commun.* **1990**, No. 19, 1374–1376.
- (10) Martin, A. S.; Sambles, J. R.; Ashwell, G. J. Molecular Rectifier. *Phys. Rev. Lett.* **1993**, *70* (2), 218–221.
- (11) Jiang, L.; Yuan, L.; Cao, L.; Nijhuis, C. A. Controlling Leakage Currents: The Role of the Binding Group and Purity of the Precursors for Self-Assembled Monolayers in the Performance of Molecular Diodes. *J. Am. Chem. Soc.* **2014**, *136* (5), 1982–1991.
- (12) Capozzi, B.; Xia, J.; Adak, O.; Dell, E. J.; Liu, Z.-F.; Taylor, J. C.; Neaton, J. B.; Campos, L. M.; Venkataraman, L. Single-Molecule Diodes with High Rectification Ratios through Environmental Control. *Nat. Nanotechnol.* **2015**, *10* (6), 522–527.
- (13) Perrin, M. L.; Galán, E.; Eelkema, R. M.; Thijssen, J.; Grozema, F.; van der Zant, H. S. J. A Gate-Tunable Single-Molecule Diode. *Nanoscale* **2016**, *8* (16), 8919–8923.
- (14) Chen, X.; Roemer, M.; Yuan, L.; Du, W.; Thompson, D.; del Barco, E.; Nijhuis, C. A. Molecular Diodes with Rectification Ratios Exceeding 10 5 Driven by Electrostatic Interactions. *Nat. Nanotechnol.* **2017**, 12 (8), 797–803.
- (15) Kong, G. D.; Jin, J.; Thuo, M.; Song, H.; Joung, J. F.; Park, S.; Yoon, H. J. Elucidating the Role of Molecule-Electrode Interfacial Defects in Charge Tunneling Characteristics of Large-Area Junctions. *J. Am. Chem. Soc.* **2018**, *140* (38), 12303–12307.
- (16) Li, M.; Tu, B.; Cui, B.; Zhao, X.; Yang, L.; Fang, Q.; Yan, Y.; Grzybowski, B. A. Efficient and Long-Lasting Current Rectification by Laminated Yet Separated, Oppositely Charged Monolayers. ACS Appl. Electron. Mater. 2019, 1 (11), 2295–2300.
- (17) Lin, J.-L.; Cao, Z.; Bai, X.; Chen, N.; Li, C.; Xiao, X.; Wang, L.; Li, Y. Molecular Diodes With Tunable Threshold Voltage Based on π -Extended Tetrathiafulvalene. *Adv. Mater. Interfaces* **2022**, 9 (27), 2201238.
- (18) Sullivan, R. P.; Morningstar, J. T.; Castellanos-Trejo, E.; Bradford, R. W.; Hofstetter, Y. J.; Vaynzof, Y.; Welker, M. E.;

- Jurchescu, O. D. Intermolecular Charge Transfer Enhances the Performance of Molecular Rectifiers. *Sci. Adv.* **2022**, 8 (31), No. eabq7224.
- (19) Metzger, R. M. Unimolecular Electronics. *Chem. Rev.* **2015**, *115* (11), 5056–5115.
- (20) Xiang, D.; Wang, X.; Jia, C.; Lee, T.; Guo, X. Molecular-Scale Electronics: From Concept to Function. *Chem. Rev.* **2016**, *116* (7), 4318–4440.
- (21) Vilan, A.; Aswal, D.; Cahen, D. Large-Area, Ensemble Molecular Electronics: Motivation and Challenges. *Chem. Rev.* **2017**, *117* (5), 4248–4286.
- (22) Yuan, L.; Nerngchamnong, N.; Cao, L.; Hamoudi, H.; del Barco, E.; Roemer, M.; Sriramula, R. K.; Thompson, D.; Nijhuis, C. A. Controlling the Direction of Rectification in a Molecular Diode. *Nat. Commun.* **2015**, *6* (1), 6324.
- (23) Lamport, Z. A.; Broadnax, A. D.; Scharmann, B.; Bradford, R. W.; DelaCourt, A.; Meyer, N.; Li, H.; Geyer, S. M.; Thonhauser, T.; Welker, M. E.; Jurchescu, O. D. Molecular Rectifiers on Silicon: High Performance by Enhancing Top-Electrode/Molecule Coupling. ACS Appl. Mater. Interfaces 2019, 11 (20), 18564–18570.
- (24) Xie, Z.; Bâldea, I.; Frisbie, C. D. Determination of Energy-Level Alignment in Molecular Tunnel Junctions by Transport and Spectroscopy: Self-Consistency for the Case of Oligophenylene Thiols and Dithiols on Ag, Au, and Pt Electrodes. *J. Am. Chem. Soc.* **2019**, *141* (8), 3670–3681.
- (25) Xie, Z.; Bâldea, I.; Frisbie, C. D. Energy Level Alignment in Molecular Tunnel Junctions by Transport and Spectroscopy: Self-Consistency for the Case of Alkyl Thiols and Dithiols on Ag, Au, and Pt Electrodes. J. Am. Chem. Soc. 2019, 141 (45), 18182–18192.
- (26) Cho, S. J.; Kong, G. D.; Park, S.; Park, J.; Byeon, S. E.; Kim, T.; Yoon, H. J. Molecularly Controlled Stark Effect Induces Significant Rectification in Polycyclic-Aromatic-Hydrocarbon-Terminated n-Alkanethiolates. *Nano Lett.* **2019**, *19* (1), 545–553.
- (27) Stark, J. Observation of the Separation of Spectral Lines by an Electric Field. *Nature* **1913**, *92* (2301), 401–401.
- (28) Sie, E. J.; Lui, C. H.; Lee, Y.-H.; Kong, J.; Gedik, N. Observation of Intervalley Biexcitonic Optical Stark Effect in Monolayer WS2. *Nano Lett.* **2016**, *16* (12), 7421–7426.
- (29) De Santis, L.; Trusheim, M. E.; Chen, K. C.; Englund, D. R. Investigation of the Stark Effect on a Centrosymmetric Quantum Emitter in Diamond. *Phys. Rev. Lett.* **2021**, *127* (14), 147402.
- (30) Liu, Y.; Qiu, Z.; Carvalho, A.; Bao, Y.; Xu, H.; Tan, S. J. R.; Liu, W.; Castro Neto, A. H.; Loh, K. P.; Lu, J. Gate-Tunable Giant Stark Effect in Few-Layer Black Phosphorus. *Nano Lett.* **2017**, *17* (3), 1970–1977.
- (31) Scolfaro, D.; Finamor, M.; Trinchão, L. O.; Rosa, B. L. T.; Chaves, A.; Santos, P. V.; Iikawa, F.; Couto, O. D. D., Jr. Acoustically Driven Stark Effect in Transition Metal Dichalcogenide Monolayers. *ACS Nano* **2021**, *15* (9), 15371–15380.
- (32) Nijhuis, C. A.; Reus, W. F.; Whitesides, G. M. Molecular Rectification in Metal-SAM-Metal Oxide-Metal Junctions. *J. Am. Chem. Soc.* **2009**, *131* (49), 17814–17827.
- (33) Kumar, S.; van Herpt, J. T.; Gengler, R. Y. N.; Feringa, B. L.; Rudolf, P.; Chiechi, R. C. Mixed Monolayers of Spiropyrans Maximize Tunneling Conductance Switching by Photoisomerization at the Molecule-Electrode Interface in EGaIn Junctions. *J. Am. Chem. Soc.* **2016**, 138 (38), 12519–12526.
- (34) Ai, Y.; Kovalchuk, A.; Qiu, X.; Zhang, Y.; Kumar, S.; Wang, X.; Kühnel, M.; Nørgaard, K.; Chiechi, R. C. In-Place Modulation of Rectification in Tunneling Junctions Comprising Self-Assembled Monolayers. *Nano Lett.* **2018**, *18* (12), 7552–7559.
- (35) Lamport, Z. A.; Broadnax, A. D.; Harrison, D.; Barth, K. J.; Mendenhall, L.; Hamilton, C. T.; Guthold, M.; Thonhauser, T.; Welker, M. E.; Jurchescu, O. D. Fluorinated Benzalkylsilane Molecular Rectifiers. *Sci. Rep.* **2016**, *6* (1), 38092.
- (36) Beebe, J. M.; Kim, B.; Gadzuk, J. W.; Daniel Frisbie, C.; Kushmerick, J. G. Transition from Direct Tunneling to Field Emission in Metal-Molecule-Metal Junctions. *Phys. Rev. Lett.* **2006**, 97 (2), 026801.

- (37) Bâldea, I. Ambipolar Transition Voltage Spectroscopy: Analytical Results and Experimental Agreement. *Phys. Rev. B* **2012**, 85 (3), 035442.
- (38) Xie, Z.; Bâldea, I.; Frisbie, C. D. Why One Can Expect Large Rectification in Molecular Junctions Based on Alkane Monothiols and Why Rectification Is so Modest. *Chem. Sci.* **2018**, *9* (19), 4456–4467.
- (39) Morikawa, T.; Tsutsui, M.; Komoto, Y.; Yokota, K.; Taniguchi, M. Dependence of Molecular Diode Behaviors on Aromaticity. *J. Phys. Chem. Lett.* **2022**, *13* (27), 6359–6366.
- (40) Scheer, E.; Cuevas, J. C. *Molecular Electronics*; World Scientific: Hackensack, NJ, 2010.
- (41) Bâldea, I. Revealing Molecular Orbital Gating by Transition Voltage Spectroscopy. *Chem. Phys.* **2010**, 377 (1), 15–20.
- (42) Zhang, G.; Ratner, M. A.; Reuter, M. G. Is Molecular Rectification Caused by Asymmetric Electrode Couplings or by a Molecular Bias Drop? *J. Phys. Chem. C* **2015**, *119* (11), 6254–6260.
- (43) Bâldea, I. Why Asymmetric Molecular Coupling to Electrodes Cannot Be at Work in Real Molecular Rectifiers. *Phys. Rev. B* **2021**, 103 (19), 195408.